

# Preparation of a new anion exchanger by pre-irradiation grafting technique and its adsorptive removal of rhenium (VII) as analogue to $^{99}\text{Tc}^*$

ZU Jian-Hua (殂建华),<sup>1</sup> WEI Yue-Zhou (韦悦周),<sup>1</sup> YE Mao-Song (叶茂松),<sup>1</sup>  
TANG Fang-Dong (唐方东),<sup>2</sup> HE Lin-Feng (何林锋),<sup>2</sup> and LIU Rui-Qin (刘瑞芹)<sup>1,†</sup>

<sup>1</sup>*School of Nuclear Science and Engineering, Shanghai Jiao Tong University, Shanghai 200240, China*

<sup>2</sup>*Shanghai Institute of Measurement and Testing Technology, Shanghai 201203, China*

(Received May 7, 2014; accepted in revised form July 7, 2014; published online December 20, 2014)

A new anion exchanger with pyridine groups was prepared by grafting of 2-vinyl pyridine onto polypropylene (PP) nonwoven fabrics by pre-irradiation grafting technique, followed by quaternization of pyridine rings in grafted chains in reaction with bromoethane. The results showed that the grafting yield increased with the monomer concentration and conversion ratio of quaternization increased with the time. The grafted and quaternized fabrics were characterized by FT-IR, DSC, SEM and ICP. The possibility of adsorption of perrhenate ( $\text{ReO}_4^-$ ), a nonradioactive analogue to pertechnetate ( $^{99}\text{TcO}_4^-$ ), from aqueous solution by anion exchanger was investigated. The experiments performed at pH= 0.1–6 showed that pH = 2.2 was the optimal acidity for  $\text{ReO}_4^-$  adsorption, and an adsorption equilibrium was achieved in 30 min. The reaction enthalpy was  $-12.55 \text{ kJ/mol}$ , indicating that the adsorption process is exothermic. XPS tests indicated that the  $\text{ReO}_4^-$  uptake was a typical ion exchange between  $\text{Cl}^-$  on anion exchanger and  $\text{ReO}_4^-$ .

Keywords: 2-vinyl pyridine, Pre-irradiation grafting, Anion exchanger, Perrhenate

DOI: [10.13538/j.1001-8042/nst.26.S10302](https://doi.org/10.13538/j.1001-8042/nst.26.S10302)

## I. INTRODUCTION

Rhenium (Re), one of the rarest metals, in abundance of just  $10^{-7}\%$  in the Earth crust, has been widely used in chemical engineering, metallurgy, aerospace and national defense. Re, placed in the VIIB group of the periodic table together with technetium (Tc), is a good chemical analogue of Tc, due to their similar electronic configuration, stereochemistry and thermodynamic properties.

$^{99}\text{Tc}$  is a  $\beta$ -emitter fission product with a half-life of  $2 \times 10^5$  years and a high fission yield (6.3% of  $^{235}\text{U}$ ) [1]. Removal of  $^{99}\text{Tc}$  from spent nuclear fuel is important because of its long lifetime, toxicity and high mobility in the environment. In the literatures, Re was usually chosen as an alternative element for radioactive  $^{99}\text{Tc}$  to avoid handling high radioactivity. This study was aimed at providing experimental data for  $^{99}\text{Tc}$  separation.

For bulk separation of Re, liquid-liquid extraction method is normally applied [2, 3]. A large amount of secondary waste, which is difficult to treat and dispose, will be generated in the liquid-liquid extraction process [4]. Therefore, new materials and methods have been developed to protect the environment and improve Re removal efficiency [5]. Adsorptive separation, using an extractant impregnated resin (EIR), was reported as a promising method to obtain high selectivity for both low and high concentration solutions, as it combines the advantages of ion exchange and extraction [6, 7]. The main disadvantage of these extractant materials, however, is their low stability due to the leakage of extractant from the

support, which results in gradual loss of their separation capacity and reduced lifetime [8]. In addition, due to absence or weak attracting tendency between the extractants and solid support, the impregnation process is carried out inadequately. These drawbacks cause to restrict application of EIR in hydrometallurgy and other industries.

Kim *et al.* demonstrated that  $\text{ReO}_4^-$ , which is often used as pertechnetate analogue, is efficiently absorbed by natural organic polymer chitosan containing amino groups [9–11]. Liang *et al.* showed that adsorption of pertechnetate by Forager sponge could be attributed to the presence of amino groups [12]. Therefore, on the basis of our previous research and literature data, it is possible to use amino-functionalized copolymers for perrhenate sorption [13, 14]. In this article, we report our work to develop an advanced ion exchanger of high stability with compacted equipment for separation of perrhenate. A new anion exchanger with a quaternary ammonium functional groups is prepared by grafting 2-vinyl pyridine (2-VP) onto polypropylene (PP) nonwoven fabrics using pre-irradiation technique and subsequent quaternization of graft copolymers by reaction with bromoethane. It was used successfully in our research for removal of perrhenate.

## II. EXPERIMENTAL

### A. Materials

PP nonwoven fabrics of  $\Phi$  10–20  $\mu\text{m}$  fibers (Shanghai Rundong Nonwoven Co., Ltd, China) were washed with acetone and vacuum dried at  $50^\circ\text{C}$ . From Shanghai Yuanqiang Chemical Reagent Co., Ltd, China, 2-vinyl pyridine was obtained.  $\text{KReO}_4$ , from Tianjin No.3 Chemistry Reagent Factory, was spectroscopically pure. *N, N*-dimethylformamide (DMF), bromoethane and other chemicals, were of analytical-reagent grade, and used as received.

\* Supported by the National Natural Science Foundation of China (No. 91226111 and 11305102) and Shanghai Science and Technology Foundation (No. 12DZ2293800)

† Corresponding author, [rqliu@sjtu.edu.cn](mailto:rqliu@sjtu.edu.cn)

## B. Equipments

The PP nonwoven fabrics were irradiated by 2 MeV electron beams at Shanghai Applied Radiation Institute, School of Environmental and Chemical Engineering, Shanghai University. The virgin, grafted and quaternized nonwoven fabrics were characterized by FT-IR spectroscopy (IR Affinity-1, Shimadzu), differential scanning calorimeter (DSC, 200PC, Netzsch) and scanning electron microscope (SEM, JSM-6700, JEOL). The metal ions concentration was measured by an inductively coupled plasma atomic emission spectrometer (Icps-7510, Shimadzu). The solution pH was determined by pH meter (PHB-4, Shanghai Leici Instrument Scientific Co. Ltd.).

## C. Preparation of anion exchanger

Figure 1 shows synthesis process of the anion exchanger prepared by radiation-induced grafting of 2-VP onto PP nonwoven fabrics and quaternization of the grafted nonwoven fabrics by reaction with bromoethane.

The PP fabrics were sealed in polyethylene bags containing high purity nitrogen and irradiated with 2 MeV 1 mA E-beams, which scanned an area of 120 cm (*l*) × 7 cm (*w*). The total absorbed dose was 100 kGy for all samples. For grafting, a Pyrex tube was added with solvent DMF and monomer 2-VP, and bubbled with nitrogen for 15 min. The pre-irradiated fabrics were immersed in the Pyrex tube, which was sealed after 5 min N<sub>2</sub> bubbling and put into a water bath at constant temperature. The grafted fabrics were washed several times with a mixture of ethanol and water (1 : 1) to remove the unreacted monomer and homopolymer on the fabrics surface. They were vacuum dried in at 60 °C up to constant weight. The grafting yield was calculated by

$$\text{Grafting yield} = [(W_g - W_0)/W_0] \times 100\%, \quad (1)$$

where  $W_g$  and  $W_0$  are the weights of PP-g-VP fabrics and the virgin, respectively.

The grafted samples were reacted with bromoethane in ethanol solution at 65 °C for several hours. They were washed several times with deionized water. The *conversion ratio* was calculated by

$$\text{Conversion ratio} = [(W_a - W_g)/(W_g - W_0)] \times (M_1/M_2) \times 100\%, \quad (2)$$

where  $W_a$  is weight of the quaternized PP-g-VP,  $M_1$  is molecular weight of the 2-VP, and  $M_2$ , the bromoethane.

## D. Adsorption experiments

The anion exchanger pre-equilibrated by 1 M HCl solution was immersed in the feed Re(VII) solution adjusted to the desired pH. The mixture, at appropriate temperature and initial ion concentration, was stirred throughout the experiment. Then, the anion exchanger was removed and the Re

concentration was measured by ICP. The adsorption amount ( $Q$ ) and distribution ratio ( $D$ ) was calculated with Eqs. (3) and (4), respectively

$$Q = \frac{(C_0 - C) \cdot V}{W}, \quad (3)$$

$$D = Q/C, \quad (4)$$

where  $Q$  is the amount of Re(VII) adsorbed on the anion exchanger (mg/g);  $C_0$  and  $C$  are concentrations of the Re (VII) before and after adsorption (ppm), respectively;  $W$  is mass of the anion exchanger (g) and  $V$  is volume of the metal ion solution (L).

## E. Characterization of the samples

### 1. DSC analysis

Changes in crystallinity and thermal behavior, induced by grafting and quaternization, were evaluated by DSC. The samples were loaded into the system at 20 °C, and experiment was run in at 20–200 °C in N<sub>2</sub> atmosphere at a heating rate of 20 °C/min. The samples fusion heat values were obtained from the area under the thermograms curves.

### 2. X-ray photoelectron spectroscopy

X-ray photoelectron spectroscopy (AXIS Ultra<sup>DLD</sup>, Shimadzu-Kratos, Japan) was applied to determine the interactions between the organic functional groups in anion exchangers and the adsorbed ReO<sub>4</sub><sup>-</sup>. The XPS spectra were obtained by applying the energy source of monochromatic Mg K<sub>α</sub> ray (1253.6 eV) at 15 kV and 10 mA. The residual pressure in the analysis-chamber was  $5 \times 10^{-8}$  Pa. The samples were scanned from 0 to 1200 eV in 80-eV steps. The elements of C, O, N and Re were measured at 282–294 eV, 528–536 eV, 396–404 eV and 43–51 eV, respectively. The spectra were decoded using the curve-fitting program with the subtraction of Shirley background and the ratio of Gaussian (0)-Lorentzian (100%).

### 3. SEM

Surface morphology of the virgin PP and grafted PP was captured with SEM. The dried samples were mounted on specimen studs and sputter coated with thin film of gold to prevent charring. Topographical images in SEM were formed from back scattered primary or low-energy secondary electrons.

### 4. FT-IR

FT-IR analysis of the PP, PS-g-VP and quaternized PS-g-VP were performed by FT-IR spectroscopy. The spectra

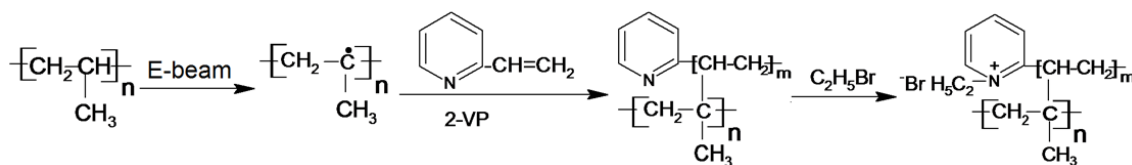


Fig. 1. Preparation of anion exchanger by radiation induced grafting and quaternization

were measured in transmission mode in range of  $1200\text{ cm}^{-1}$  to  $1800\text{ cm}^{-1}$ .

### III. RESULTS AND DISCUSSION

#### A. Effect of reaction time on grafting yield at different monomer concentrations

Figure 2 shows that the grafting yield increases rapidly with reaction time up to 180 min, where it tends to level off; while it always increases with monomer concentration. The grafting depends largely on the monomers available to the radical sites in the nonwoven fabrics. A higher monomer concentration means a greater availability of 2-VP in the fabrics; but with a too long reaction time, some radicals are inactivated and monomers tend to homopolymerize, which affects diffusion rate of monomers, hence the decrease of grafting rate and slow increase of grafting yield.

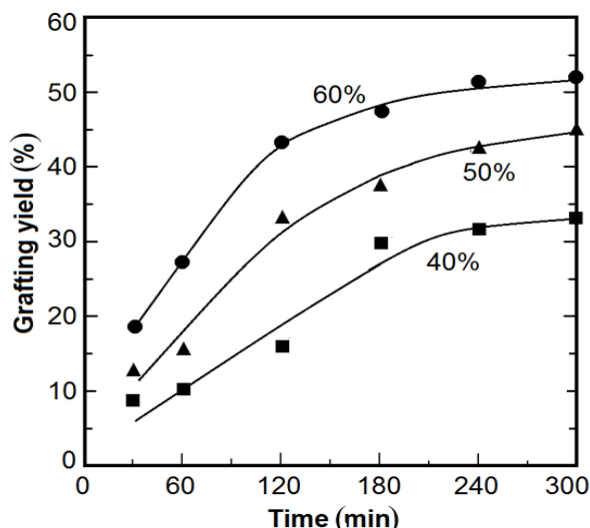


Fig. 2. The grafting yield vs. reaction time at various monomer concentrations. The samples were irradiated to 100 kGy and grafted at  $50^\circ\text{C}$  in DMF solvent.

#### B. Effect of quaternization time on conversion ratio

The conversion ratio in  $65^\circ\text{C}$  quaternization, as function of quaternization time, is shown in Fig. 3. It increases with up to 48 h, where it begins to level off.

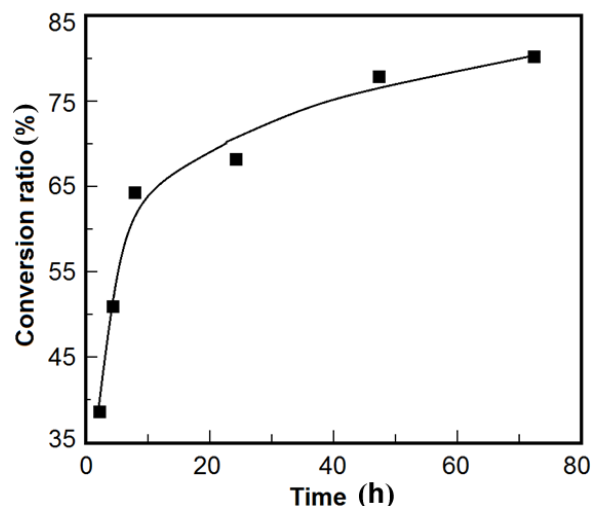


Fig. 3. The conversion ratio vs. time of quaternization at  $65^\circ\text{C}$ . The PP-g-VP fabrics samples were of 47.4% grafting yield.

#### C. Samples characterization

Structural changes of the nonwoven fabrics, grafted with 2-VP and quaternized with bromoethane, were analyzed by FT-IR. Fig. 4 shows FT-IR spectra of the virgin PP (a), quaternized PP-g-VP (b) and PP-g-VP (c). The absorption peaks at  $1592$  and  $1558\text{ cm}^{-1}$  in Spectrum (c) are attributed to stretching vibration of  $\text{C}=\text{N}$  in grafted 2-VP, and the peaks at  $1434$  and  $1475\text{ cm}^{-1}$  are due to stretching of  $\text{C}=\text{C}$  of pyridine ring. After quaternization, a new peak at  $1630\text{ cm}^{-1}$  is observed in Spectrum (b), showing that the nitrogen atom in pyridine ring is positively charged. Moreover, the peaks at  $1592$  and  $1558\text{ cm}^{-1}$ , related to  $\text{C}=\text{N}$  groups, becomes weak. These indicate the introduction of quaternary amine groups onto the graft chains of PP-g-AN.

Figure 5 shows DSC curves of the virgin PP (a), 26.9% PP-g-VP (b), 47.6% PP-g-VP (c) and quaternized PP-g-VP (d). Although the shape of the thermograms, for all the samples, remains almost identical, the peaks intensity decreases with increasing grafting yield. The fusion heat ( $\Delta H_m$ ) values, obtained from areas under the thermograms curves, were 70.15, 63.75, 50.32 and  $24.88\text{ J/g}$  for curves (a), (b), (c) and (d), respectively. Also, the  $\Delta H_m$  and melting point ( $T_m$ ) decrease with increasing grafting yield. The grafting took place by incorporation of amorphous polyvinyl pyridine chains in the noncrystalline region of the PP nonwoven fabrics. The grafted polyvinyl pyridine chains thereby exerted a dilution

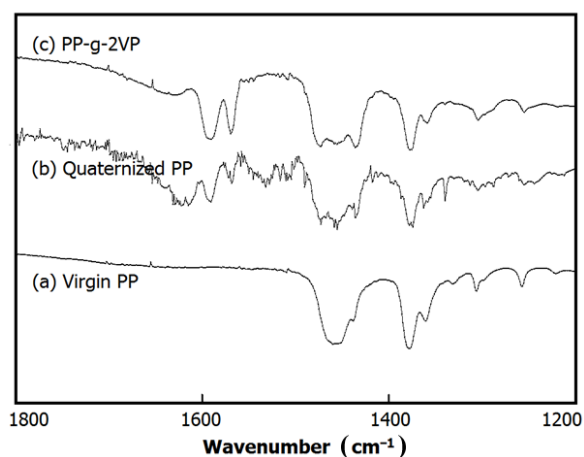


Fig. 4. FTIR spectra of the virgin PP, PP-g-2VP (grafting yield: 47.4%), and quaternized PP (conversion rate: 38.5%).

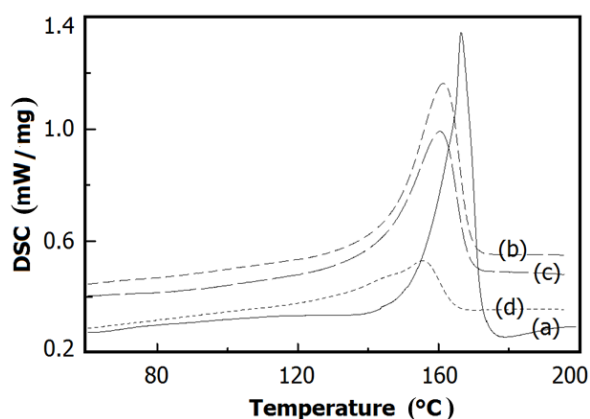


Fig. 5. DSC curves of the virgin PP (a), PP-g-2VP with grafting yield of 26.9% (b), PP-g-2VP with grafting yield of 47.4% (c) and quaternized PP-g-2VP with conversion ratio of 78.7% (d).

effect on the inherent crystallinity of the PP fabrics. Crystallinity of the grafted fabric decreased with increasing grafting yield, hence the decreased  $\Delta H_m$  with increasing grafting yield. For grafted or quaternized samples, the melting point ( $T_m$ ) is lower than the virgin fabrics. The existence of graft chains hinders the formation of big size crystallite. Small crystallites usually melt at lower temperature than big ones.

Surface morphology of the virgin PP (a) and 51.2.0% PP-g-VP (b) are shown in Fig. 6. The fibers became thicker after grafting, and fabrics surface became rougher, due to growth of the graft chains.

#### D. Adsorption ability

##### 1. Effect of pH on adsorption amount

The pH effects on the adsorption of Re(VII) are shown in Fig. 7. It can be seen that Re(VII) is adsorbed poorly on

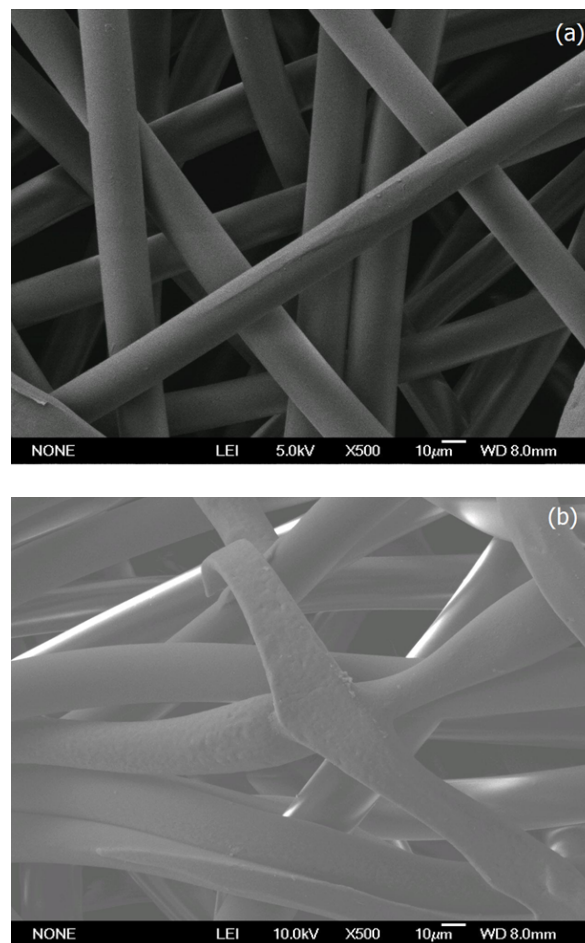


Fig. 6. SEM images of the virgin PP (a) and PP-g-VP with grafting yield of 50.3% (b).

the anion exchanger at lower pH ( $\text{pH} < 0.5$ ), and adsorption amount increases sharply with pH value up to pH 2.2, where it begins to decrease.

The result explains the phenomenon of decrease in adsorption amount with increasing concentration of hydrochloric acid by competitive adsorption reaction of  $\text{ReO}_4^-$  and  $\text{Cl}^-$  on anion exchanger. At low pH value ( $\text{pH} < 0.5$ ), the  $\text{Cl}^-$  concentration is high, the competitive effect of  $\text{Cl}^-$  with  $\text{ReO}_4^-$  for the quaternary amine groups on the anion exchanger is significant, which reduces the electrostatic attraction to  $\text{ReO}_4^-$ ; whereas high pH ( $\text{pH} > 2.2$ ) is not conducive to the protonation of tertiary amines, which do not react with bromoethane during quaternization reaction, and exchangeable groups on anion exchanger become less, hence the decreased adsorption amount.

##### 2. Effect of anion exchanger concentration in solution on adsorption efficiency

Figure 8 shows the relationship between anion exchanger concentration in solution and adsorption efficiency. The ad-

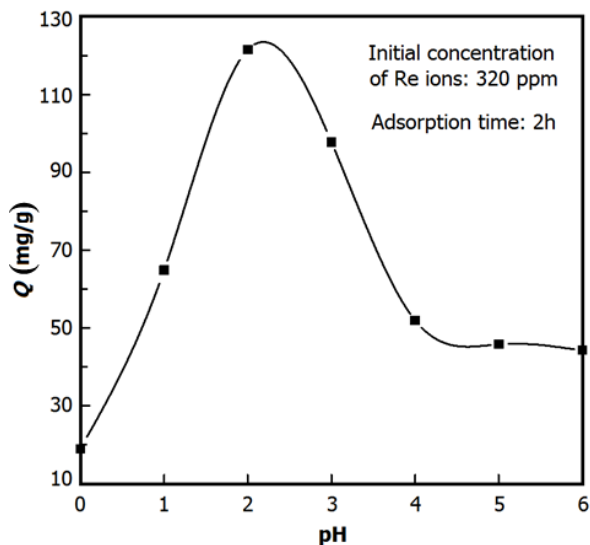


Fig. 7. Effect of pH on the adsorption amount.

sorption efficiency increases with anion exchanger concentration and levels off towards 98.1%. Apparently, the optimum adsorption concentration is 8 mg/mL for a constant Re(VII) ion initial concentration 320 ppm.

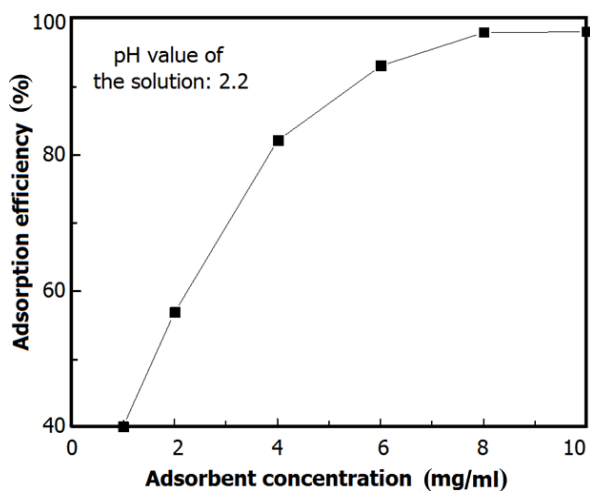


Fig. 8. Adsorption efficiency as function of adsorbent concentration.

### 3. Calculation of adsorption rate constant

Using constant anion exchanger concentration, the concentration of Re(VII) ions in the solution was determined at different times. As shown in Fig. 9, the adsorption of Re(VII) ions reached an equilibrium value in 30 min. The results can be described by the adsorption Eq. (5) [15]:

$$-\ln(1 - Q/Q_e) = kt + c, \quad (5)$$

where  $Q_e$  is the adsorption amount of Re(VII) ions at equilibrium time,  $t$  is the adsorption time,  $k$  is the adsorption constant rate, and  $c$  is a constant. The results can be converted into the plot  $-\ln(1 - Q/Q_e)$  vs.  $t$  as shown in the insert of Fig. 9. The linear relationship indicates that the liquid film diffusion controls speed of the adsorption process [16]. The adsorption rate constant of Re(VII) ions calculated from the slope in the insert is  $3.81 \times 10^{-3} \text{ s}^{-1}$ .

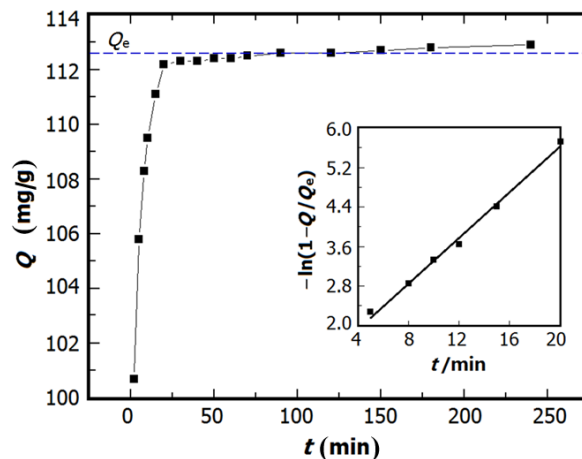
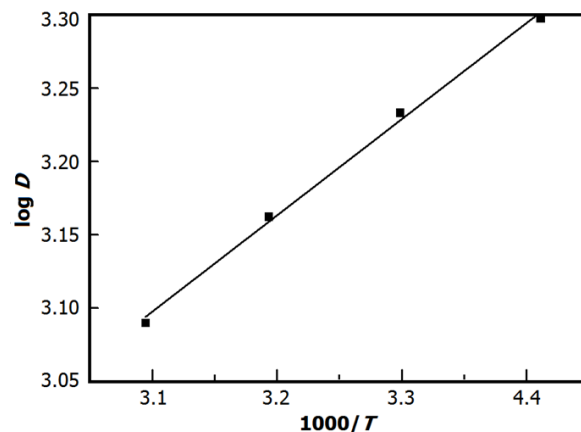


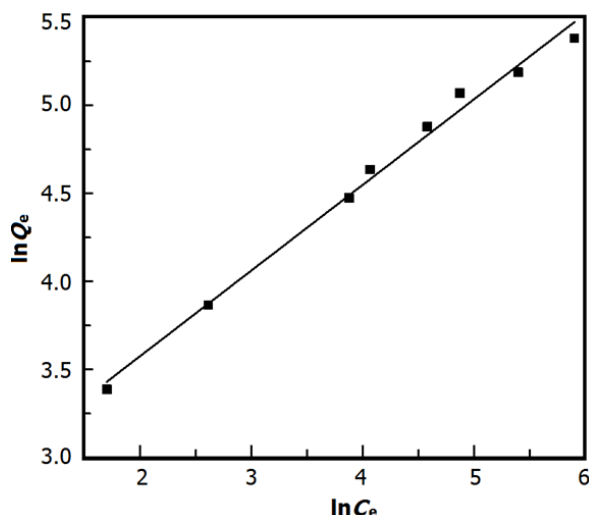
Fig. 9. Effect of adsorption time on adsorption amount. Initial Re ions concentration: 320 ppm; pH: 2.2.

### 4. Effect of temperature on adsorption amount

The temperature effect on the adsorption amount of Re(VII) ions were studied at 20–50 °C. The data of  $\log D$  vs.  $1000/T$  are plotted in Fig. 10, where  $D$  was obtained by calculating the experimental data with Eq. (4). Using the slope of Fig. 10 and the Van't Hoff equation,  $\partial(\log D)/\partial(1/T) = -\Delta H/(2.303R)$ , the adsorption enthalpy of Re(VII) ions was  $\Delta H = -12.55 \text{ kJ/mol}$ , which means that the adsorption process is an exothermic reaction for the adsorption of Re(VII) ions onto the anion exchanger.

Fig. 10. Plot of  $\log D$  vs.  $1000/T$ .



Fig. 11. Plot of  $\ln Q_e$  vs.  $\ln C_e$ .

#### 5. Effect of the initial concentration of Re(VII) ions on adsorption amount

By changing the initial concentration of Re(VII) ions, at constant pH and adsorption temperature, a series of  $C_e$  were obtained when the adsorption reached equilibrium, and the corresponding equilibrium adsorption amount ( $Q_e$ ) was obtained. When adsorption achieved saturation, the Freundlich equation  $\ln Q = (\ln C_e)/n + \ln K$  was used to clarify the adsorption mechanism. The plot of  $\ln Q_e$  vs.  $\ln C_e$  (Fig. 11) shows a linear relationship, indicating that the adsorption behavior of exchanger fits Freundlich equation. The slope ( $1/n$ ) is 0.487, and  $1/n < 0.5$  means that the adsorptivity of the anion exchanger for Re(VII) is a facile process.

#### 6. Reusability of anion exchanger

To evaluate the reusability of the anion exchanger, adsorption-desorption cycles were repeated three times. The adsorbed Re(VII) ions were easily desorbed by 3 mol/L hydrochloric acid solution at room temperature during 1 h and under stirring. The adsorption amounts of anion exchanger of the 1<sup>st</sup>, 2<sup>nd</sup> and 3<sup>rd</sup> adsorption-desorption cycle were respectively 123.8, 20.7 and 117.0 mg/g, showing a slight decrease with a loss of adsorption amount about 2.5–5.5% in the three cycles. The results indicate that the anion exchanger had good performance of reusability.

#### 7. XPS analysis of adsorption of Re(VII) onto anion exchanger

Samples of anion exchangers before and after  $\text{ReO}_4^-$  adsorption were evaluated by XPS technique, aimed at studying the shifts of binding energy of different atoms. Binding energies of C, O and N in anion exchanger, and C, O, N and Re in

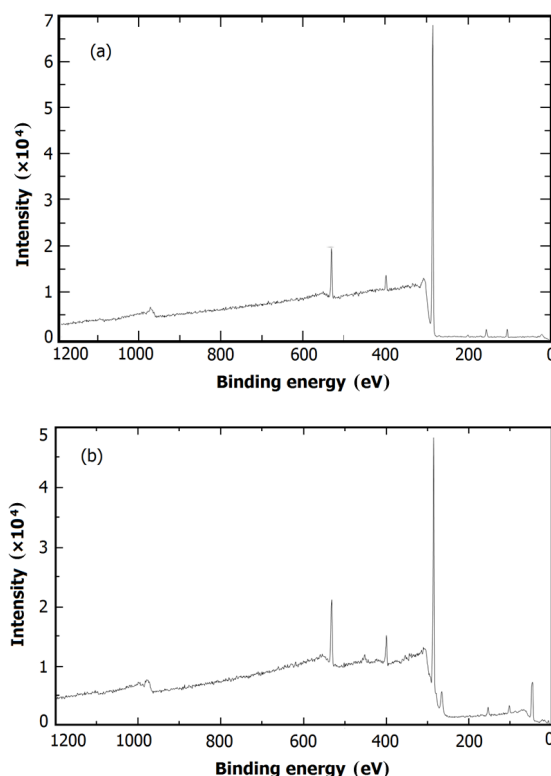


Fig. 12. XPS spectra of anion exchanger before (a) and after (b) Re adsorption.

anion exchanger after binding  $\text{ReO}_4^-$  are shown in Fig. 12. The N1s before adsorption of  $\text{ReO}_4^-$ , was at 399.1 eV, and after that it was 398.7 eV, virtually no change could be observed, indicating that the nature of rhenium uptake is typical ion exchange between  $\text{Cl}^-$  on anion exchanger and  $\text{ReO}_4^-$ . The new peak at 45.43 eV, in Fig. 12(b), is assigned to Re 4f in  $\text{ReO}_4^-$ , showing that Re (VII) is adsorbed onto anion exchanger.

## IV. CONCLUSION

The new type of anion exchanger with a quaternary ammonium functional groups was prepared by grafting of 2-VP onto PP nonwoven fabrics by pre-irradiation technique, followed by quaternization of the graft copolymers through reaction with bromoethane. The results show that the grafting yield increases with the monomer concentrations, and conversion ratio of quaternization increases with the time. FT-IR and DSC characterizations of the grafted and quaternized fabrics confirm that expected functional groups are anchored onto PP nonwoven fabrics.

The anion exchanger has maximum adsorption amount of rhenium ions at pH 2.2. The adsorption process is an exothermic reaction, so the adsorption of rhenium ions can be carried out at low temperatures. The adsorption behavior, of the anion exchanger for Re(VII), can be described with the Langmuir equation. XPS tests indicate that the nature of Rhenium uptake was a typical ion exchange driven by the electrostatic

attraction. The adsorption rate constant is  $3.81 \times 10^{-3} \text{ s}^{-1}$ . The adsorbed rhenium ions can be easily desorbed by 3 M

HCl, and the anion exchanger is of good reusability. The adsorption amount of anion exchanger decreases slightly after adsorption-desorption of three cycles.

- 
- [1] Lieser K H. Technetium in the nuclear fuel cycle, in medicine and in the environment. *Radiochim Acta*, 1993, **63**: 5–8.
- [2] Cao Z, Zhong H, Qiu Z H. Solvent extraction of rhenium from molybdenum in alkaline solution. *Hydrometallurgy*, 2009, **97**: 153–157. DOI: [10.1016/j.hydromet.2009.02.005](https://doi.org/10.1016/j.hydromet.2009.02.005)
- [3] Fang D W, Gu X J, Xiong Y. Thermodynamics of solvent extraction of rhenium with trioctyl amine. *J Chem Eng Data*, 2010, **55**: 424–427. DOI: [10.1021/je900402w](https://doi.org/10.1021/je900402w)
- [4] Miniakhmetov I A, Semenov S A, Musatova V Y. Solvent extraction of rhenium with N-(2-hydroxy-5-nonylbenzyl)-beta-hydroxyethylmethylamine. *Russ J Inorg Chem*, 2013, **58**: 1380–1382. DOI: [10.1134/S0036023613110144](https://doi.org/10.1134/S0036023613110144)
- [5] Yan Y, Yi M, Zhai M L, Ha H F, *et al.* Adsorption of  $\text{ReO}_4^-$  ions into polyDMAEMA hydrogels prepared by UV-induced polymerization. *React Funct Polym*, 2004, **59**: 149–154. DOI: [10.1016/j.reactfunctpolym.2004.01.004](https://doi.org/10.1016/j.reactfunctpolym.2004.01.004)
- [6] Moon J K, Han Y J, Jung C H. Adsorption of rhenium and rhodium in nitric acid solution by Amberlite XAD-4 impregnated with Aliquat 336. *Korean J Chem Eng*, 2006, **23**: 303–308. DOI: [10.1007/BF02705732](https://doi.org/10.1007/BF02705732)
- [7] Bartosova A, Rajec P, Reich M. Preparation and characterization of an extraction chromatography column for technetium separation based on Aliquat-336 and silica gel support. *J Radioanal Nucl Chem*, 2004, **261**: 119–124. DOI: [10.1023/B:JRNC.0000030944.93883.58](https://doi.org/10.1023/B:JRNC.0000030944.93883.58)
- [8] Trochimczuk A, Kabay N, Arda M. Stabilization of solvent impregnated resins (SIRs) by coating with water soluble polymers and chemical crosslinking. *React Funct Polym*, 2004, **59**: 1–7. DOI: [10.1016/j.reactfunctpolym.2003.12.011](https://doi.org/10.1016/j.reactfunctpolym.2003.12.011)
- [9] Kim E, Benedetti M, Boulegue F. Removal of dissolved rhenium by sorption onto organic polymers: study of rhenium as an analogue of radioactive technetium. *Water Res*, 2004, **38**: 448–454. DOI: [10.1016/j.watres.2003.09.033](https://doi.org/10.1016/j.watres.2003.09.033)
- [10] Lou Z N, Zhao Z Y, Li Y X. Contribution of tertiary amino groups to Re (VII) biosorption on modified corn stalk: Competitiveness and regularity. *Bioresource Technol*, 2013, **133**: 546–554. DOI: [10.1016/j.biortech.2013.01.165](https://doi.org/10.1016/j.biortech.2013.01.165)
- [11] Jia M, Cui H M, Jin W Q. Adsorption and separation of rhenium (VII) using N-methylimidazolium functionalized strong basic anion exchange resin. *J Chem Tech Biotech*, 2013, **88**: 437–443. DOI: [10.1002/jctb.3904](https://doi.org/10.1002/jctb.3904)
- [12] Gu B H, Dowlen K E, Liang L Y. Efficient separation and recovery of Tc-99 from contaminated ground water. *Separ Technol*, 1996, **6**: 123–132. DOI: [10.1016/0956-9618\(96\)00147-6](https://doi.org/10.1016/0956-9618(96)00147-6)
- [13] Kosandrovich E G and Soldatov V S. *Fibrous Ion Exchangers and Ion Exchange Technology*, Fibrous ion exchangers and ion exchange technology. Springer Science Business Media, 2012, 299–371.
- [14] Plevaka A V, Troshkina I D, Zemskova L A, *et al.* Rhenium sorption by fibrous chitosan-carbon materials. *Russ J Inorg Chem*, 2009, **54**: 1168–1171. DOI: [10.1134/S0036023609070286](https://doi.org/10.1134/S0036023609070286)
- [15] Body G E, Adamson A W, Myers L S. The exchange adsorption of ions from aqueous solutions by organic zeolites, II: kinetics. *J Am Chem Soc*, 1947, **69**: 2836–2848.
- [16] Shu Z N and Yang M H. Adsorption of rhenium (VII) with anion exchange resin D318. *Chin J Chem Eng*, 2011, **18**: 372–377. DOI: [10.1016/S1004-9541\(10\)60233-9](https://doi.org/10.1016/S1004-9541(10)60233-9)